Journal of Cell Science

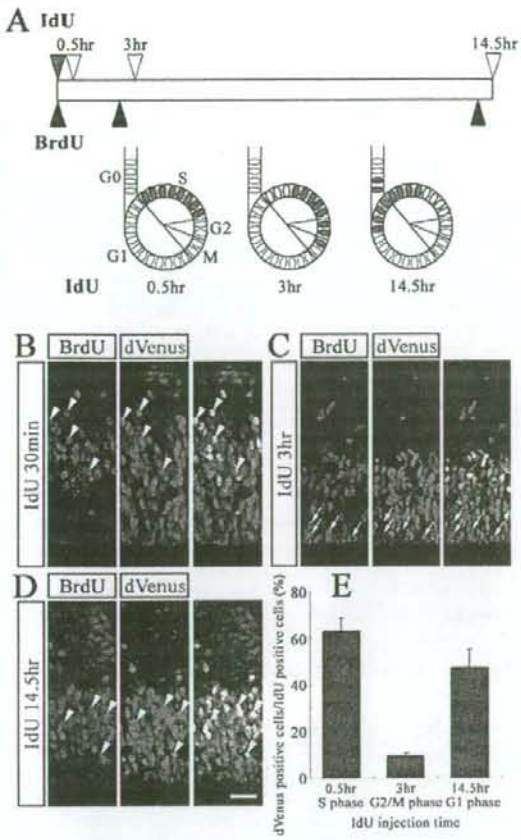

Fig. 2. Cell-cycle-dependent expression of *Nes*. (A) Schematic diagram of the timing used to administer thymidine analogues to label cells in each cell-cycle phase (see Materials and Methods for details). (B-D) IdU (red) was injected for 0.5 hour (B), 3 hours (C) and 14.5 hours (D) to label cells in S, G2-M and G1 phases, respectively. BrdU (purple) was injected 30 minutes before sacrifice to label cells in S phase. dVenus (green) was expressed in many of the cells in G1 and S phase (arrowheads), but cells in the G2-M phase were mostly dVenus negative (arrows). (E) Ratio of IdU-positive cells that expressed dVenus to the total number of IdU-positive cells, counted for each cell-cycle phase. Cells in G1 and S phase expressed the highest levels of dVenus, whereas its expression levels were much lower during G2-M phase. Scale bar: 25 μm (B-D). Data represent the mean ± s.e.m.

(n=4). Immunostaining for phospho-histone H3 further demonstrated the lack of dVenus expression in M-phase cells (Fig. 3C). Thus, *Nes* expression is high in G1 phase during process extension, and it is lost in G2-M phase, which is characterized by the adventricular nuclear movement and rounding up of the soma.

Phosphorylation of Brn2 on Ser362 reduces Brn2 binding to DNA and lowers the expression of *Nes* during G2-M

We next addressed the underlying molecular mechanism of the cell-cycle-dependent regulation of *Nes*. We first investigated whether the responsible transcription factors were expressed in a cell-cycle-dependent manner. Immunohistochemical analysis for SOX1-SOX3 and class III POU transcription factor (Pou3f2 or Brn2) showed them to be expressed ubiquitously throughout the VZ (Fig. 4A), indicating that dVenus was expressed only in a subset of these SOX- or POU-expressing cells. This result led us to consider whether post-translational modification of the transcription factors might contribute to the cyclic changes in dVenus expression.

Phosphorylation inhibits the DNA-binding activity of POU proteins such as Oct1 and GHF1 (Pit1) during G2-M (Kapiloff et al., 1991; Segil et al., 1991; Caelles et al., 1995), and the phospho-acceptor site is highly conserved in all POU-domain proteins. This site corresponds to Ser362 in Brn2. Therefore, we next asked whether the phosphorylation of Brn2 increased during G2-M in vitro. 293T cells expressing Flag-tagged Brn2 or Brn2 S362A, in which Ser362 is replaced by alanine, were synchronized at G1, S and G2-M phases (supplementary material Fig. S3), and labeled with [^{32}P]orthophosphate (GE Healthcare) for the 6 hours preceding harvest. The level of Brn2 phosphorylation was low in G1 (Fig. 4B lane 1) and S (Fig. 4B lane 2) phases, but it increased as the cells progressed through the cycle to G2-M phase (Fig. 4B lane 3). By contrast, the phosphorylation level of Brn2 S362A remained constant, showing essentially the same level in G2-M (Fig. 4B lane 5) as in G1 (Fig. 4B lane 4). These results indicate that Brn2 is phosphorylated on Ser362, in a cell-cycle-dependent manner, during G2-M phase.

To investigate the relationship between the phosphorylation of Brn2 and *Nes* expression, we next introduced a phosphorylation-mimicking point mutation that substituted Asp for Ser at Brn2 Ser362. We first used this construct in luciferase reporter assays (Fig. 4C). An octamerized 30-mer nestin core enhancer (Nes30) (Tanaka et al., 2004), which includes the SOX- and POU-binding sites, was fused to the rabbit β-globin minimal promoter and inserted into the pGL3 basic luciferase reporter vector. When SOX2 was expressed alone, Nes30 was weakly activated (4.5-fold). The expression of Brn2 alone led to stronger activation (8.6-fold). By contrast, Brn2 S362D increased reporter expression only slightly, to twice the basal level. When SOX2 and Brn2 were expressed together, Nes30 activity increased dramatically (24.5-fold). This synergistic action, consistent with a previous report (Tanaka et al., 2004), remarkably reduces when Brn2 was replaced with Brn2 S362D in the same experiment. The Nes30 activity increase (5-fold) was the same as for SOX2 alone (Fig. 4C).

This effect of expressing phospho-mimicking Brn2 on Nes30 activity could be caused by a decreased binding affinity for DNA or by instability of the phosphorylated Brn2. We performed an electrophoretic mobility shift assay (EMSA) to discriminate between these possibilities, using the Nes30 sequence probe and whole-cell lysates of 293T cells overexpressing Flag-tagged Brn2 or Brn2 S362D. The amount of Brn2 S362D binding complex was significantly reduced (Fig. 4D black arrow; lane 3), compared with that of wild-type Brn2 (Fig. 4D black arrow; lane 2). To ascertain whether the binding to Nes30 was Brn2 specific, an anti-Flag antibody was added to the binding reactions in a super-shift assay, which showed specific binding of the Flag-tagged Brn2 (Fig. 4D black arrowhead; lanes 4, 5). No binding reaction was observed in lysates of untransfected 293T cells (Fig. 4D lane 1), and no significant difference was seen between the stability of Brn2 and phospho-mimicking Brn2 S362D (Fig. 4E lane 2, 3), normalized to the expression of α-tubulin (Fig. 4E, *), consistent with the uniform expression pattern of Brn2 in the VZ in vivo (Fig. 4A). These results strongly suggested that the reduction of *Nes* expression

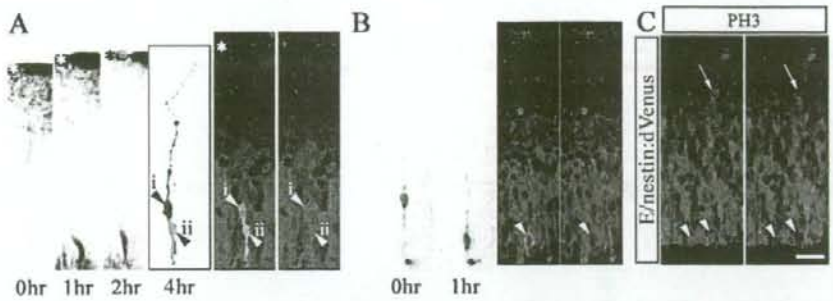

Fig. 3. The relationship between *Nes* expression levels and the 3D morphology of neural progenitor cells. (A) VZ cells were labeled with DiI (red) from the pial surface and observed for 4 hours after mitosis. The radial fiber, which became extremely thin during mitosis, was inherited by one of the daughter cells (arrowhead i). Four hours after mitosis, both daughter cells expressed dVenus. Within this period, the cell that inherited the process thickened its fiber and extended 20 μm (arrowhead i), whereas the cell that did not inherit the fiber began to elaborate its own process (arrowhead ii). (B) During G2 phase, the VZ progenitor cells possessed a mature fiber, and each nucleus migrated toward the ventricular surface. dVenus was not expressed in the cells during this phase (arrowhead). (C) Cells in M phase, labeled with phospho-histone H3 (PH3), were dVenus-negative both near the ventricular surface (arrowheads) and in the subventricular zone (arrow). The asterisk indicates the pial surface. Scale bar: 25 μm (A-C).

during G2-M phase is due to the decreased binding affinity of phosphorylated Brn2 for the *Nes* core enhancer element. Therefore, we conclude that the phosphorylation of POU transcription factors downregulates the cell-cycle-dependent expression of *Nes*.

Discussion

E/nestin:dVenus transgenic mice as a versatile model system

GFP and its variants are widely used as reporters for gene expression, lineage tracing and protein localization studies. The stability of GFP allows its accumulation and enables it to be detected easily in living cells. However, this stability also limits its application in studies requiring rapid reporter turnover. The transgenic mice reported here, which express a fluorescent reporter with a short half-life, showed the strict localization of dVenus to the VZ, which contains neural progenitors (Fig. 1C), and its expression pattern was mutually exclusive with that of an early neuronal marker, β-tubulin III (Fig. 1D). In transgenic mice carrying an EGFP reporter under the same regulatory sequence (Kawaguchi et al., 2001), the fluorescent signal was still detectable after cells had differentiated into neurons (Fig. 1D). Therefore, the novel transgenic mouse expressed dVenus in the desired pattern, but with a half-life that restricted its expression to neural progenitors. Our novel transgenic mice also allowed us to prospectively isolate self-renewable and multipotent neural stem cells using flow cytometry (supplementary material Fig. S2), and real-time quantitative PCR analysis showed that the dVenus reporter fluorescence intensity accurately reflected the relative expression levels of *Nes* mRNA (Fig. 1G). These results confirmed the utility of this reporter system. We then used this system to trace changes in the transcription of *Nes* in vivo during the cell cycle.

Relationship between SOX-POU signaling and the maintenance of neural progenitor cells

The SOX family of HMG-box transcription factors is a key regulator of embryonic development and cell-fate determination. In certain cases, SOX1-SOX3 interact with various partner transcription factors and participate in defining distinct cell states that depend on the partner factors, such as Pax6 in lens differentiation, Oct3/4 in establishing the epiblast/ES cell state and Brn2 in the neural primordium (Kamachi et al., 2000; Tanaka et al., 2004). Although SOX1-SOX3 are known to suppress neurogenesis by maintaining neural progenitor cells in an undifferentiated state in the vertebrate CNS (Bylund et al., 2003), the responsible target gene has not been identified. Since *Nes* is a target gene of SOX and POU transcription factors (Tanaka et al., 2004), we monitored its expression pattern to learn more about the contribution of SOX proteins to the maintenance of the neural progenitor cell state. We found that the expression of *Nes*, as represented by the fluorescence intensity of dVenus, reflected its activation by a SOX-POU complex (supplementary material Fig. S1). We also found that transcription by the SOX-POU complex was inactivated during G2-M (Figs 2, 3) by the cell-cycle-dependent phosphorylation of the POU transcription factor (Fig. 4). Our data suggest that the cell-fate choice to remain an undifferentiated neural progenitor cell, regulated by the SOX-POU complex, is completed during G1 to S phase. Interestingly, the activation of Notch1 (indicated by its nuclear localization), which maintains neural progenitor cells in the undifferentiated state by inducing Hes1/5 expression (Gaiano and Fishell, 2002), also takes place in G1 to S phase (Tokunaga et al., 2004). However, it is still unclear whether cells that have been stimulated with SOX-POU during the early G1 phase can change their cell fate decision and differentiate into neurons without further progression of the cell cycle. Therefore, future research needs to address the timing of the cell-fate decision during G1 phase of daughter cells. Our present study demonstrates that the target genes of the SOX-POU transcription factor complex are regulated in a more complicated manner than expected (Tanaka et al., 2004), and it provides a model for further understanding the contribution of SOX transcription factors to the maintenance of neural progenitor cells in an undifferentiated state.

Cell-cycle-dependent expression of nestin

By allowing mouse cells to incorporate thymidine analogues at different times before sacrifice, we confirmed that *Nes* expression was regulated in a cell-cycle-dependent manner in vivo (Fig. 2). Moreover, in vitro experiments suggested that the weak *Nes* expression during G2-M could be attributed to the cell-cycle-dependent phosphorylation of Brn2 (Fig. 4B). This phosphoacceptor

Journal of Cell Science

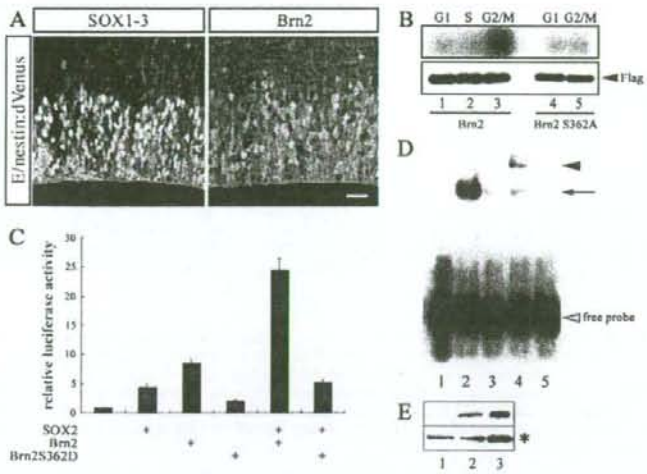

Fig. 4. The expression of *Nes* is reduced by the decreased affinity of Brn2 phosphorylated on Ser362 for the *Nes* core enhancer during G2-M. (A) Immunostaining showed that only a subset of SOX1-SOX3 and Brn2 immunopositive cells expressed dVenus in the E14.5 cerebral cortex. (B) Flag-tagged Brn2- and Brn2-S362A-expressing 293T cells were synchronized at the G1, S and G2-M phases and labeled with [^{32}P]orthophosphate. The low level of Brn2 phosphorylation at G1 and S (lane 1, 2) increased during the G2-M phase (lane 3). However, the phosphorylation level of Brn2 S362A at G2-M (lane 5) was the same as in the G1 phase (lane 4). (C) SOX2, Brn2 and Brn2 S362D were used to transfect cells either alone, or as a SOX-POU combination, with a luciferase-encoding reporter plasmid carrying an octamerized nestin core enhancer sequence (8×Nes30). Together, SOX2 and Brn2 synergistically activated the 8×Nes30 reporter. By contrast, when Brn2 was replaced with Brn2 S362D, the activation was markedly lower. Data represent means ± s.e.m. (D) EMSA showing the lower binding affinity of Brn2 S362D (lane 3) compared with the wild-type Brn2 (lane 2) for the Nes30 probe (black arrow). The binding specificity was confirmed by a super shift assay (black arrowhead; lanes 4, 5). No binding reaction was seen with the lysate of untransfected 293T cells (lane 1). Open arrowhead indicates the free probe. (E) Western blot showing the Brn2 and Brn2 S362D input used for the EMSA. No significant difference was seen between the stability of Brn2 and Brn2 S362D when normalized to α-tubulin expression (*). Scale bar: 25 μm.

site at Brn2 Ser362 is highly conserved in all POU-domain proteins, and other POU proteins, such as Oct1 and GHF1 (Pit1), are phosphorylated on the same site during G2-M (Kapiloff et al., 1991; Segil et al., 1991; Caelles et al., 1995). In agreement, our data showed a marked decrease in reporter activity from the *Nes* core enhancer when Asp was substituted for Brn2 Ser362 (Fig. 4C). By EMSA, we demonstrated that the reduced transcription was due to a dramatic drop in Brn2 S362D binding of the *Nes* core enhancer, compared with wild-type Brn2 (Fig. 4D). Our hypothesis that cell-cycle-dependent Brn2 phosphorylation regulates *Nes* expression is based on in vitro studies, and we have not characterized the kinase responsible for this regulation. However, because Cdc2 mitotic kinase, which is ubiquitously expressed in all cells during G2-M phase, is a candidate kinase for the cell-cycle-dependent phosphorylation of Oct1 and GHF1 (Segil et al., 1991; Caelles et al., 1995), it is reasonable to expect that Brn2 is subject to the same regulatory mechanism in the developing brain in vivo.

Physiological relevance of nestin in neural progenitor cells in vivo

In spite of the numerous IF family members, the expression of IFs exhibits a high degree of cell-type specificity (Herrmann and Aebi, 2004). The unique physical properties and interaction capabilities of these distinct IF molecules with accessory proteins mediate the generation of a highly dynamic and interconnected cell-type-specific cytoarchitecture. In the CNS, undifferentiated progenitor cells express nestin and vimentin. During neural differentiation, nestin is downregulated and displaced with the expression of neurofilament (NF) proteins and/or peripherin in neurons, and GFAP in astrocytes (Lariviere and Julien, 2003). Although many of the gene-targeting approaches of the neural IF genes demonstrate mild phenotypes, substantial developmental loss of motor axons was detected in mice lacking NF-L and in NF-M–NF-H double knockout mice. Mice lacking NF-L also had a scarcity of IF structures and exhibited a severe axonal hypotrophy (Lariviere and Julien, 2003). In GFAP and vimentin double-deficient mice, the post-traumatic glial scarring was looser and less organized (Pekny et al., 1999). This evidence supports a role for IFs in cytogenesis and stabilization.

Nestin cannot form filaments of its own, but it can readily form copolymer IFs when combined with vimentin both in vivo and in vitro (Marvin et al., 1998; Steinert et al., 1999). A complex of nestin-vimentin heterodimers is less stable than vimentin homopolymers when subjected to increasing concentrations of urea in vitro (Steinert et al., 1999). Therefore, nestin can retain the flexibility of the IF network in neural progenitor cells. It has been reported that the pial process of neural progenitor cells exhibits a coiled or hairpin-loop structure that produces a spring-like force, which functions to propel the cell soma away from the proliferating VZ (Miyata and Ogawa, 2007). Since the IF network has been shown to have a vital role for this twisting of the process (Miyata and Ogawa, 2007), nestin can enable the neural progenitor cell to possess this complicated architecture. This assumption is supported by the fact that the IF network depolymerizes during M phase, requiring the twisting process to take place during G1 phase when the *Nes* transcription is most prominent (Fig. 2).

Furthermore, nestin has been reported as a potential target of cyclin-dependent kinase 5 (Cdk5) and phosphorylation may target it for subsequent ubiquitylation and degradation outside the VZ (Sahlgren et al., 2003). In the Cdk5-deficient cortex, nestin expression persisted in cortical neurons (Cicero and Herrup, 2005), suggesting that the post-translational modification fine-tunes the expression of nestin. Since Cdk5 is predominantly observed outside the VZ, phosphorylation of nestin must take place after the transcriptional shutdown (Fig. 1D). Interestingly, transcription of *Nes* is also downregulated in G2-M (Fig. 2) when Cdc2 phosphorylates nestin (Sahlgren et al., 2001; Chou et al., 2003), suggesting that the transcription and post-translational modification is precisely orchestrated.

Correlation between *Nes* expression and morphological change in neural progenitor cells in vivo

The reduction in the binding activity of transcription factors during G2-M might be a general event that frees chromatin during mitosis.

Journal of Cell Science

However, we also found that the molecular regulation of *Nes* correlated with changes in the 3D morphology of the neural progenitor cell in vivo. During the transition from M to G1, the process of the progenitor cell becomes extremely thin. Simultaneously, mitosis-specific phosphorylation promotes disassembly of the IF network (Yasui et al., 2001; Sahlgren et al., 2001; Noctor et al., 2002; Chou et al., 2003). Although the thin fiber is retained during M phase and inherited by only one of the daughter cells (Fig. 3A), both daughter cells must reorganize their cytoskeleton during G1 to S phase, either to extend a new process or to thicken the inherited one and elongate it to match the increasing width of the cerebral wall. Even if the nestin protein is stable and is divided equally between the daughter cells, it must double in quantity to effect this network-remodeling step. In addition, this cyclical regulation of *Nes* transcription provides nestin concomitant with the elongation of the radial fiber in G1 to S phase (Fig. 2 and Fig. 3A), which must happen at each division because of the continuous thickening of the cerebral wall (Takahashi et al., 1993). Moreover, it is interesting that the length of G1 phase extends during development (Takahashi et al., 1995), simultaneously with the requirement for a longer process, as the cerebral wall thickens (Takahashi et al., 1993).

In addition to nestin being supplied when needed for process elongation, the dramatic decline in *Nes* expression during G2 phase, when neural progenitor cells possess a thick and matured process, is also crucial for normal morphological dynamics (Fig. 2 and Fig. 3B,C). It is known that nestin disassembles the IFs through phosphorylation during the transition from M to G1 (Sahlgren et al., 2001; Chou et al., 2003). However, an extremely high dosage of nestin can also disassemble the IFs physically (Steinert et al., 1999), irrespective of its phosphorylation state. Thus, the reduction of *Nes* transcription in G2-M phase is essential, once the progenitor cell obtains a mature IF network, for preserving the appropriate timing of IF disassembly. Furthermore, an attractive hypothesis is that the expression of *Nes* correlates with the cell-cycle-dependent migration of the nuclei, described as interkinetic nuclear movement (Sauer and Walker, 1959; Fujita, 1962). Recently, several groups proposed that microtuble- and actin-dependent mechanisms are important for the adventricular nuclear movement in G2 phase. Knockdown of LIS1 (Tsai et al., 2005), myosin II (Tsai et al., 2007), Cep120 and transforming acid coiled-coil proteins (TACCs) (Xie et al., 2007) impaired the migration of the nuclei towards the ventricular surface without affecting the bipolor morphology of the neural progenitor cell. By contrast, the mechanism of migrating away from the ventricular surface in G1 phase, which is slower than the adventricular migration (Takahashi et al., 1995), remains unknown. Because of the synchronization of *Nes* transcription and the nuclear movement, nestin could be involved not only in the extension of the progenitor cell, but also the nuclear movement in G1 phase. Building on previously reported results showing that IF depolymerization creates abnormal neural progenitor cell morphology (Miyata and Ogawa, 2007), our present study, which accurately maps the expression profile of *Nes*, strongly suggests that not only post-translational modification but also precise transcriptional regulation are vital for (1) maintaining the 3D morphology of neural progenitor cells and (2) their mitotic cycle, through remodeling of the cytoskeletal network in vivo (Fig. 5).

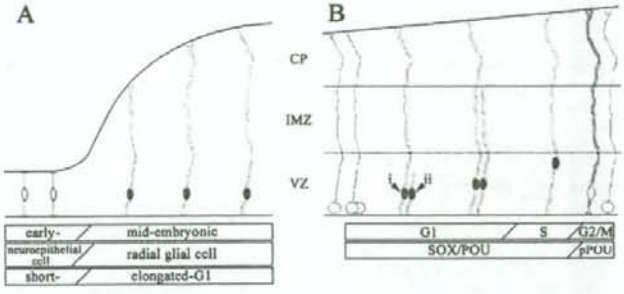

Fig. 5. A schematic diagram of *Nes* expression according to the cell-cycle-dependent morphological changes of neural progenitor cells in the developing cerebral cortex. (A) A schematic diagram of the stage-dependent thickening of the mouse cerebral wall based on Takahashi et al. (Takahashi et al., 1993). Cortical progenitor cells elongate as development proceeds from an early 'neuroepithelial cell' to a mid-embryonic 'radial glial cell' stage. The expression of *Nes* (green) was strong during the neurogenic stage, which accompanied obvious cerebral wall thickening and the prolonged G1 phase. (B) Cell-cycle-dependent morphological changes of mid-embryonic progenitor cells. At the beginning of the G1 phase, each progenitor cell generated at the ventricular surface is either connected to the pial surface (cell i) or lacking a pial process (cell ii). The daughter cell that inherited the pial process (cell i) elongates its process within a single cell cycle to match the cerebral wall thickening. The other daughter cell (cell ii) elaborates a new pial process, mainly during G1, and adopts the bipolar radial glial morphology by S phase. During mitosis, the cell body rounds up and the process becomes extremely thin. A model for the lineage-restriction of the progenitor cell is omitted for simplification. The expression of *Nes* (green) was observed concomitant with the elongation of the radial process during the G1 to S phases. At G2-M, *Nes* expression declined because of the phosphorylation of its upstream regulator class III POU protein, allowing the cells to undergo mitosis. Note that the duration of each cell cycle phase illustrated (G1, S, and G2-M) is according to those determined at E14 by Takahashi et al. (Takahashi et al., 1995). CP, cortical plate; IMZ, intermediate zone; VZ, ventricular zone.

Materials and Methods

Production of transgenic mice

The 637 bp (1162-1798) fragment of the second intronic region of rat *Nes* with the minimum promoter of heat shock protein 68 (hsp68) from the nestin-hsp68-EGFP plasmid (Kawaguchi et al., 2001) was subcloned into the *AseI-BamHI* site of pd4EGFP-N1 (BD Biosciences, San Jose, CA). The gene for Venus was inserted into this plasmid in place of that for EGFP. The purified transgene was microinjected into the pronucleus of fertilized mouse eggs. Four independent lines showing identical expression patterns were generated in a C57BL/6 background. The data presented are from experiments using heterozygous mice from a single line. All procedures were performed in accordance with institutional guidelines. The date of conception was established by the presence of a vaginal plug and recorded as E0.5.

Immunohistochemistry and immunocytochemistry

Post-fixed mouse embryo brains were embedded in 3% LMP Agarose (Invitrogen, Carlsbad, CA) and sectioned at 50 μm on a vibratome (VT1000; Leica, Heidelberg, Germany). Free-floating sections were washed twice with 0.1 M phosphate-buffered saline, pH 7.4 (PBS) and blocked with blocking solution (PBS containing 5% normal donkey serum and 0.3% Triton X-100; Sigma-Aldrich, St Louis, MO) for 30 minutes. Subsequently, sections were incubated overnight at 4°C in a mixture of the primary antibodies described above, in blocking solution. After washing three times with PBS, sections were reacted with secondary antibodies at room temperature for 2 hours, washed three more times, and then coverslipped. Immunostained sections were observed with a confocal laser-scanning microscope LSM510 META (Zeiss, Jena, Germany). dVenus fluorescence was readily detectable in fixed sections. However, when the counterstaining antibody required some pretreatment of the sections, dVenus was immunostained with a rabbit anti-GFP antibody. Sorted cells were spun down immediately onto poly-L-ornithine (15 μg/ml) and fibronectin (1 μg/ml) coated coverslips and immunostained by standard procedures. Post-stained cells were observed under a fluorescence microscope (Axiophoto; Zeiss). Primary antibodies against nestin (Rat401; Developmental Studies Hybridoma Bank of Iowa University), β-tubulin III, GFAP (Sigma), O4 (Chemicon, Temecula, CA), GFP (MBL, Woburn,

MA), Brn2 (Santa Cruz Biotechnology, Santa Cruz, CA), phospho-histone H3 (Cell Signaling Technology, Danvers, MA) and Group B1 SOX [SOX1-3; a kind gift from H. Kondoh, Ohsaka University (Tanaka et al., 2004)] were used according to the manufacturers' protocols.

Flow cytometry

The cerebral wall of E14.5 transgenic or wild-type mouse embryos was dissected out into a chilled Hank's buffered saline solution, and suspended by brief mechanical treatment. One μg/ml of propidium iodide (PI) was added and the cells were filtered through a nylon mesh. Cell sorting and analysis were performed using MoFlo (Cytomation, Fort Collins, CO) with Summit software. Cells were analyzed for forward scatter, side scatter, PI fluorescence and dVenus or EGFP fluorescence with an argon laser (488 nm, 100 mW). Dead cells were excluded by gating on forward and side scatter, and by eliminating PI-positive events. Viable cells from the transgenic mice were sorted into ice-cold culture medium. Cells harvested from wild-type mice were used to set the background fluorescence.

Determination of cell-cycle kinetics

Timed-pregnant female mice bearing transgenic embryos expressing dVenus were given thymidine analogues (50 μg/g body weight of the pregnant mouse) by intraperitoneal injection. The thymidine analogues, 5-bromo-2′-deoxyuridine (BrdU) and 5-iodo-2′-deoxyuridine (IdU) (Sigma-Aldrich), are incorporated into cells during the S phase of the cell cycle. The length of each cell-cycle stage in the dorsomedial region of the E14.5 mouse embryo was reported previously (Takahashi et al., 1995). On the basis of this report, we identified the cells that were labeled with IdU injected 3 hours before sacrifice as being in the G2-M phase. To overcome potential confusion from the long half-life of IdU, and to eliminate the labeling of cells remaining in G2-M phase, cells in the G1 phase were labeled with IdU 14.5 hours before sacrifice, when all the labeled cells had left the ventricular surface. Cells in the S phase were labeled by injecting BrdU 30 minutes before sacrifice in each trial. To detect BrdU and IdU, sections were pretreated with 2 M HCl for 5 minutes at room temperature, neutralized with 0.1 M Tris-HCl (pH 8.8) for 10 minutes, washed three times with PBS, and treated as described above for immunological staining from the blockage step. To detect IdU, an antibody that crossreacts with BrdU (Invitrogen) was used. The BrdU signal was distinguished from the IdU signal with an anti-BrdU-specific antibody (Abcam, Cambridge, MA).

Reporter assays

An octamerized Nes30 sequence was fused to rabbit β-globin minimal promoter and inserted into the pGL3-Basic (Promega, Madison, WI) reporter vector. For reporter assays, NIH3T3 cells were cotransfected with 0.6 μg reporter, 10 ng effecter and reference pEF-LacZ (0.6 μg) using Lipofectamine Plus (Invitrogen). The amount of transfected DNA was equalized with empty vectors.

Electrophoretic mobility shift assay

Flag-tagged Brn2 and Brn2 S362D were overexpressed in 293T cells. After 2 days, whole-cell lysates were prepared in a lysis buffer containing 10 mM Tris-HCl (pH 7.6), 50 mM NaCl, 30 mM sodium phosphate, 50 mM sodium fluoride, 20 mM β-glycerophosphate, 1% Triton X-100 and protease inhibitor mixture (Complete; Roche Applied Science, Basel, Switzerland). The sense and antisense Nes30 sequences were annealed and labeled with [γ-^{32}P]ATP (GE Healthcare, Piscataway, NJ) as a probe. The binding reaction was performed in a total volume of 25 μl binding buffer (50 mM HEPES-KOH pH 7.8, 250 mM KCl, 5 mM EDTA pH 8.0, 25 mM $MgCl_2$, 50% glycerol, and 25 mM DTT). Cell lysates were incubated for 30 minutes at room temperature with the labeled oligonucleotides. For the supershift assay, the binding product was incubated with an antibody against Flag (Sigma) for another 30 minutes. The samples were separated on native 8% polyacrylamide gels at 20 mA in Tris-borate EDTA buffer.

Slice culture and DiI labeling

Slice culture and DiI labeling were performed as reported previously (Miyata et al., 2004). The cerebral cortex of E14.5 E/nestin:dVenus transgenic mouse embryos was labeled with DiI from the pial surface and sliced into coronal sections. Sections were embedded in collagen gel for time-lapse recording. The cultured slices were fixed in 4% paraformaldehyde for 15 minutes, vibratome sectioned and subjected to confocal microscopy to observe the dVenus expression in DiI-labeled cells.

We thank Hisato Kondoh for providing the rabbit anti-SOX1-3 antibody, Masaharu Ogawa for the Brn2 expression vector, and Miho Ohsugi for technical advice. This work was supported by a grant-in-aid from the Japanese Ministry of Education, Science, Sports and Culture of Japan (MEXT) and a grant from SORST, Japan Society for the Promotion of Science to H.O., the 21st Century COE program of MEXT to Keio University, and a grant from Bridgestone Corporation to K.S.

References

Bylund, M., Andersson, E., Novitch, B. G. and Muhr, J. (2003). Vertebrate neurogenesis is counteracted by Sox1-3 activity. *Nat. Neurosci.* **6**, 1162-1168.

Caelles, C., Hennemann, H. and Karin, M. (1995). M-phase-specific phosphorylation of the POU transcription factor GHF-1 by a cell cycle-regulated protein kinase inhibits DNA binding. *Mol. Cell. Biol.* **15**, 6694-6701.

Chou, Y. H., Khuon, S., Herrmann, H. and Goldman, R. D. (2003). Nestin promotes the phosphorylation-dependent disassembly of vimentin intermediate filaments during mitosis. *Mol. Biol. Cell* **14**, 1468-1478.

Cicero, S. and Herrup, K. (2005). Cyclin-dependent kinase 5 is essential for neuronal cell cycle arrest and differentiation. *J. Neurosci.* **25**, 9658-9668.

Corish, P. and Tyler-Smith, C. (1999). Attenuation of green fluorescent protein half-life in mammalian cells. *Protein Eng.* **12**, 1035-1040.

Fujita, S. (1962). Kinetics of cellular proliferation. *Exp. Cell Res.* **28**, 52-60.

Gaiano, N. and Fishell, G. (2002). The role of notch in promoting glial and neural stem cell fates. *Annu. Rev. Neurosci.* **25**, 471-490.

Hayes, N. L. and Nowakowski, R. S. (2000). Exploiting the dynamics of S-phase tracers in developing brain: interkinetic nuclear migration for cells entering versus leaving the S-phase. *Dev. Neurosci.* **22**, 44-55.

Herrmann, H. and Aebi, U. (2004). Intermediate filaments: molecular structure, assembly mechanism, and integration into functionally distinct intracellular Scaffolds. *Annu. Rev. Biochem.* **73**, 749-789.

Hinds, J. W. and Ruffett, T. L. (1971). Cell proliferation in the neural tube: an electron microscopic and golgi analysis in the mouse cerebral vesicle. *Z. Zellforsch. Mikrosk. Anat.* **115**, 226-264.

Hockfield, S. and McKay, R. D. (1985). Identification of major cell classes in the developing mammalian nervous system. *J. Neurosci.* **5**, 3310-3328.

Josephson, R., Muller, T., Pickel, J., Okabe, S., Reynolds, K., Turner, P. A., Zimmer, A. and McKay, R. D. (1998). POU transcription factors control expression of CNS stem cell-specific genes. *Development* **125**, 3087-3100.

Kamachi, Y., Uchikawa, M. and Kondoh, H. (2000). Pairing SOX off: with partners in the regulation of embryonic development. *Trends Genet.* **16**, 182-187.

Kapiloff, M. S., Farkash, Y., Wegner, M. and Rosenfeld, M. G. (1991). Variable effects of phosphorylation of Pit-1 dictated by the DNA response elements. *Science* **253**, 786-789.

Kawaguchi, A., Miyata, T., Sawamoto, K., Takashita, N., Murayama, A., Akamatsu, W., Ogawa, M., Okabe, M., Tano, Y., Goldman, S. A. et al. (2001). Nestin-EGFP transgenic mice: visualization of the self-renewal and multipotency of CNS stem cells. *Mol. Cell. Neurosci.* **17**, 259-273.

Kohyama, J., Tokunaga, A., Fujita, Y., Miyoshi, H., Nagai, T., Miyawaki, A., Nakao, K., Matsuzaki, Y. and Okano, H. (2005). Visualization of spatiotemporal activation of Notch signaling: live monitoring and significance in neural development. *Dev. Biol.* **286**, 311-325.

Lariviere, R. C. and Julien, J. P. (2003). Functions of intermediate filaments in neuronal development and disease. *J. Neurobiol.* **58**, 131-148.

Lendahl, U., Zimmerman, L. B. and McKay, R. D. (1990). CNS stem cells express a new class of intermediate filament protein. *Cell* **60**, 585-595.

Li, X., Zhao, X., Fang, Y., Jiang, X., Duong, T., Fan, C., Huang, C. C. and Kain, S. R. (1998). Generation of destabilized green fluorescent protein as a transcription reporter. *J. Biol. Chem.* **273**, 34970-34975.

Lothian, C. and Lendahl, U. (1997). An evolutionarily conserved region in the second intron of the human nestin gene directs gene expression to CNS progenitor cells and to early neural crest cells. *Eur. J. Neurosci.* **9**, 452-462.

Marvin, M. J., Dahlstrand, J., Lendahl, U. and McKay, R. D. (1998). A rod end deletion in the intermediate filament protein nestin alters its subcellular localization in neuroepithelial cells of transgenic mice. *J. Cell Sci.* **111**, 1951-1961.

Miyata, T. and Ogawa, M. (2007). Twisting of neocortical progenitor cells underlies a spring-like mechanism for daughter-cell migration. *Curr. Biol.* **17**, 146-151.

Miyata, T., Kawaguchi, A., Okano, H. and Ogawa, M. (2001). Asymmetric inheritance of radial glial fibers by cortical neurons. *Neuron* **31**, 727-741.

Miyata, T., Kawaguchi, A., Saito, K., Kawano, M., Muto, T. and Ogawa, M. (2004). Asymmetric production of surface-dividing and non-surface-dividing cortical progenitor cells. *Development* **131**, 3133-3145.

Nagai, T., Ibata, K., Park, E. S., Kubota, M., Mikoshiba, K. and Miyawaki, A. (2002). A variant of yellow fluorescent protein with fast and efficient maturation for cell-biological applications. *Nat. Biotechnol.* **20**, 87-90.

Noctor, S. C., Flint, A. C., Weissman, T. A., Dammerman, R. S. and Kriegstein, A. R. (2001). Neurons derived from radial glial cells establish radial units in neocortex. *Nature* **409**, 714-720.

Noctor, S. C., Flint, A. C., Weissman, T. A., Wong, W. S., Clinton, B. K. and Kriegstein, A. R. (2002). Dividing precursor cells of the embryonic cortical ventricular zone have morphological and molecular characteristics of radial glia. *J. Neurosci.* **22**, 3161-3173.

Okano, H. (2002). Stem cell biology of the central nervous system. *J. Neurosci. Res.* **69**, 698-707.

Pekny, M., Johansson, C. B., Eliasson, C., Stakeberg, J., Wallen, A., Perlmann, T., Lendahl, U., Betsholtz, C., Berthold, C. H. and Frisen, J. (1999). Abnormal reaction to central nervous system injury in mice lacking glial fibrillary acidic protein and vimentin. *J. Cell Biol.* **145**, 503-514.

Rakic, P. (1972). Mode of cell migration to the superficial layers of fetal monkey neocortex. *J. Comp. Neurol.* **145**, 61-83.

Rakic, P. (2003). Elusive radial glial cells: historical and evolutionary perspective. *Glia* **43**, 19-32.

Reynolds, B. A. and Weiss, S. (1996). Clonal and population analyses demonstrate that an EGF-responsive mammalian embryonic CNS precursor is a stem cell. *Dev. Biol.* **175**, 1-13.

Sahlgren, C. M., Mikhailov, A., Hellman, J., Chou, Y. H., Lendahl, U., Goldman, R. D. and Eriksson, J. E. (2001). Mitotic reorganization of the intermediate filament protein nestin involves phosphorylation by cdc2 kinase. *J. Biol. Chem.* **276**, 16456-16463.

Sahlgren, C. M., Mikhailov, A., Vaittinen, S., Pallari, H. M., Kalimo, H., Pant, H. C. and Eriksson, J. E. (2003). Cdk5 regulates the organization of Nestin and its association with p35. *Mol. Cell. Biol.* **23**, 5090-5106.

Sauer, M. E. and Walker, B. E. (1959). Radiographic study of interkinetic nuclear migration in the neural tube. *Proc. Soc. Exp. Biol. Med.* **101**, 557-600.

Segil, N., Roberts, S. B. and Heintz, N. (1991). Mitotic phosphorylation of the Oct-1 homeodomain and regulation of Oct-1 DNA binding activity. *Science* **254**, 1814-1816.

Steinert, P. M., Chou, Y. H., Prahlad, V., Parry, D. A., Marekov, L. N., Wu, K. C., Jang, S. I. and Goldman, R. D. (1999). A high molecular weight intermediate filament-associated protein in BHK-21 cells is nestin, a type VI intermediate filament protein. Limited co-assembly in vitro to form heteropolymers with type III vimentin and type IV alpha-internexin. *J. Biol. Chem.* **274**, 9881-9890.

Takahashi, T., Nowakowski, R. S. and Caviness, V. S., Jr (1993). Cell cycle parameters and patterns of nuclear movement in the neocortical proliferative zone of the fetal mouse. *J. Neurosci.* **13**, 820-833.

Takahashi, T., Nowakowski, R. S. and Caviness, V. S., Jr (1995). The cell cycle of the pseudostratified ventricular epithelium of the embryonic murine cerebral wall. *J. Neurosci.* **15**, 6046-6057.

Tanaka, S., Kamachi, Y., Tanouchi, A., Hamada, H., Jing, N. and Kondoh, H. (2004). Interplay of SOX and POU factors in regulation of the Nestin gene in neural primordial cells. *Mol. Cell. Biol.* **24**, 8834-8846.

Tokunaga, A., Kohyama, J., Yoshida, T., Nakao, K., Sawamoto, K. and Okano, H. (2004). Mapping spatio-temporal activation of Notch signaling during neurogenesis and gliogenesis in the developing mouse brain. *J. Neurochem.* **90**, 142-154.

Tsai, J. W., Chen, T., Kriegstein, A. and Valle, R. B. (2005). LIS1 RNA interference blocks neural stem cell division, morphogenesis, and motility at multiple stages. *J. Cell Biol.* **170**, 935-945.

Tsai, J. W., Bremner, K. H. and Valle, R. B. (2007). Dual subcellular roles for LIS1 and dynein in radial neuronal migration in live brain tissue. *Nat. Neurosci.* **10**, 970-979.

Xie, Z., Moy, L., Sanada, K., Zhou, Y., Buchman, J. and Tsai, L. (2007). Cep120 and TACCs control interkinetic nuclear migration and the neural progenitor pool. *Neuron* **56**, 79-93.

Yasui, Y., Goto, H., Matsui, S., Manser, E., Lim, L., Nagata, K.-i. and Inagaki, M. (2001). Protein kinases required for segregation of vimentin filaments in mitotic process. *Oncogene* **20**, 2868-2876.

Zimmerman, L., Parr, B., Lendahl, U., Cunningham, M., McKay, R., Gavin, B., Mann, J., Vassileva, G. and McMahon, A. (1994). Independent regulatory elements in the nestin gene direct transgene expression to neural stem cells or muscle precursors. *Neuron* **12**, 11-24.

Journal of Cell Science